Chapter 18

Modeling of a Thermoelectric Generator Device

Eurydice Kanimba and Zhiting Tian

Additional information is available at the end of the chapter

http://dx.doi.org/10.5772/65741

Abstract

Thermoelectric generators (TEGs) are devices that employ Seebeck effect in thermopile to convert temperature gradient induced by waste heat into electrical power. Recently, TEGs have enticed increasing attention as green and flexible source of electricity able to meet wide range of power requirements from thermocouple sensors to power generators in satellites. Thermoelectric generators suffer from low-conversion efficiency; however, they could be promising solutions, when they are used to harvest waste heat coming from industry processes or central-heating systems. This chapter covers the working principles behind TEGs, depicts numerous schematics explaining functionality of TEGs, and investigates performance of TEGs. A detailed derivation process, which provides performance expressions dictating operation of TEGs, is exposed in this chapter. In addition, thermal resistance network is shown to explain thermal connection of thermocouples in TEGs in parallel and electrical connection of thermocouples in series. Performance features shown in this chapter are power output, efficiency, and voltage induced within TEG as functions of numerous parameters.

Keywords: Seebeck effect, Peltier effect, Thomson effect, Joule heating, thermal resistance network, electrical resistance network, structure of TEGs, TEGs performance expressions derivation, analytical model, performance analysis of TEGs

1. Introduction

Increase in greenhouse gases emissions in the atmosphere due to burning of fossil fuels for the production of electricity and heat energy has motivated the development of alternative efficient and clean-energy-generation systems including that for the recovery of waste heat into electrical power. Numerous power-generation systems, such as solar panels, wind turbines, and geothermal power plants, which utilize renewable energies, have been designed to reduce dependency on fossil fuels, thus reducing greenhouse gases emissions. However, such power-generation systems require high maintenance and are often expensive as compared to thermoelectric generator devices (TEGs). Thermoelectric generator device (TEG) is a device that directly converts heat into electricity. Essentially, TEG is thermoelectric module (TEM), which

consists of thermopiles, that is, a set of thermocouples built by legs of p- and n-type semiconductors, which are connected electrically in series and thermally in parallel [1, 2]. Thermocouples built by legs of p- and n-type semiconductors are sandwiched between two ceramic plates, which are to be held at two different temperatures to realize generation regime. Temperature gradient induced between top and bottom ceramic plates originates voltage on TEG poles due to Seebeck effect in thermocouples built by legs of p- and n-type semiconductors.

Employing waste heat as heat source for TEGs is cost-effective due to waste heat being free of charge and already available. About 70% of the world energy production is known to be wasted into atmosphere through heat dissipation, which is one of significant contributions in global warming [3]. Therefore, the utilization of waste heat by converting into electricity using TEGs can contribute to energy savings and preservation of the environment as well. Thermoelectric device can also operate in reverse mode as thermoelectric cooler (TEC) and produce reverse temperature gradient between top and bottom ceramic plates due to Peltier effect, if electrical bias is applied. Depending on operation mode, applying bias voltage to thermoelectric module (TEM) and hence initiating flow of electrical current result in the production of temperature difference between top and bottom plates and TEM acts as thermoelectric cooler (TEC) and vice versa; the placement of TEM in temperature gradient results in the occurrence of voltage on TEM poles and TEM acts as heat pump with the function of thermoelectric generator (TEG) [4].

Thermoelectric devices possess various advantages compared to other power-generation systems [5]. TEGs are branded attractive power-generation systems, because they are silent solid-state devices with no moving parts, environmental friendly, scalable from small to giant heat sources, and highly reliable. They also have extended lifetime and ability to utilize low-grade thermal energy to generate electrical energy.

2. TEG-working principle

2.1. Seebeck effect

Seebeck effect describes the induction of voltage, when junctions of two different conducting materials are maintained at different temperatures as shown in **Figure 1**. Seebeck effect increases in magnitude, when Seebeck coefficient of conducting materials and/or temperature difference between their connections increases. Voltage induced through Seebeck effect is defined as below:

$$V = \alpha \Delta T, \tag{1}$$

where α is Seebeck coefficient and ΔT is the temperature difference between hot junction and cold junction.

2.2. Peltier effect

Peltier effect describes heat dissipation or absorption at the connection of two conducting materials, when current flows through the junction as shown in **Figure 2**. Depending on the direction of current flow, heat is either absorbed or dissipated at connection.

http://dx.doi.org/10.5772/65741

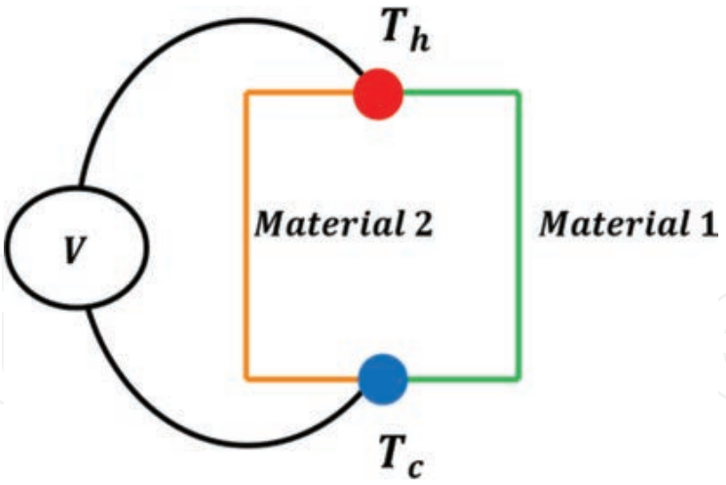

Figure 1. Seebeck effect.

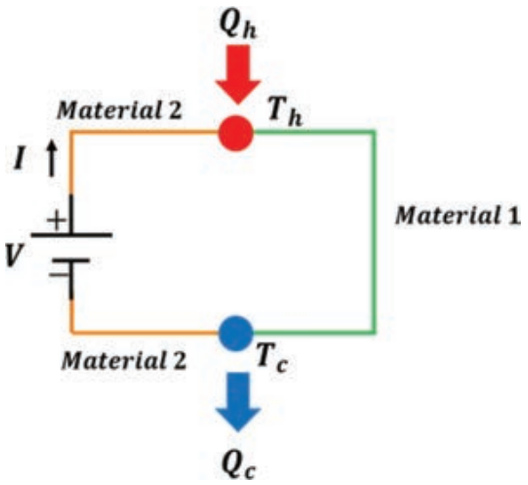

Figure 2. Peltier effect.

2.3. Thomson effect

Thomson effect describes the dissipation or absorption of heat, when electric current passes through a circuit composed of a single material, which has temperature variation along its length, as shown in **Figure 3**. ΔQ represents heat dissipation, when electrical current flows through a homogeneous conductor. Thomson coefficient is given by second Kelvin relationship [6–9]:

$$\mu = T\frac{d\alpha}{dT}, \tag{2}$$

where μ and T, respectively, symbolize Thomson coefficient and temperature. If Seebeck coefficient, α, is temperature independent, then Thomson coefficient is equal to zero.

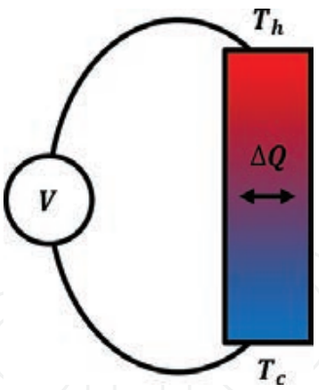

Figure 3. Thomson effect.

2.4. Joule heating

Joule-heating effect defines heat dissipated by material with nonzero electrical resistance in the presence of electrical current, as shown in **Figure 4**,

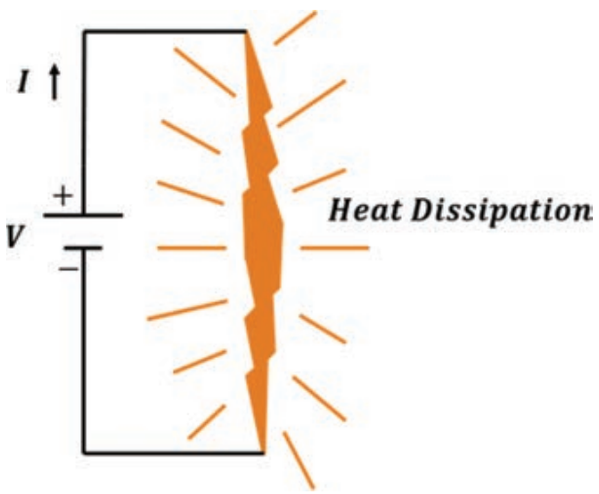

Figure 4. Joule heating.

3. Structure of TEG

3.1. Three-dimensional representation of comprehensive operation of TEG

TEGs are composed of numerous legs (slabs) made of p- and n-type semiconductors forming thermocouples, all connected electrically in series and thermally in parallel. Semiconductor legs are connected to each other through conductive copper tabs, and they are sandwiched between two ceramic plates, which conduct heat, but behave as insulators to electrical current. Schematic diagram of three-dimensional (3-D) multielement thermoelectric generator is shown in **Figure 5**.

Waste heat from various sources, such as automobile engines exhaust, industry and infrastructure-heating activities, geothermal, and others, can be supplied to top ceramic plate of TEGs.

http://dx.doi.org/10.5772/65741

As shown in **Figure 5**, heat flows through ceramic plate and copper-conductive tabs before reaching the top surface of p- and n-type legs made of proper semiconductors, which is defined as the hot side of TEG. Heat flows through both semiconductor's legs and then again through copper-conductive tabs and bottom ceramic plate. Through heat sink, the bottom ceramic plate is maintained at significantly lower temperature than top ceramic in order to produce high-temperature gradient, which will lead to high-power output. Allowed temperature applied on top and bottom ceramic plates depends on materials of p- and n-type legs. Also, p- and n-type materials are designed to possess low thermal conductivity in order to restrict, as much as possible, heat flow through semiconductors and maintain temperature difference between hot and cold sides of TEG.

Pictorial distribution of temperature along legs of TEG at conditional difference of temperature ΔT between hot and cold sides is shown in **Figure 6**.

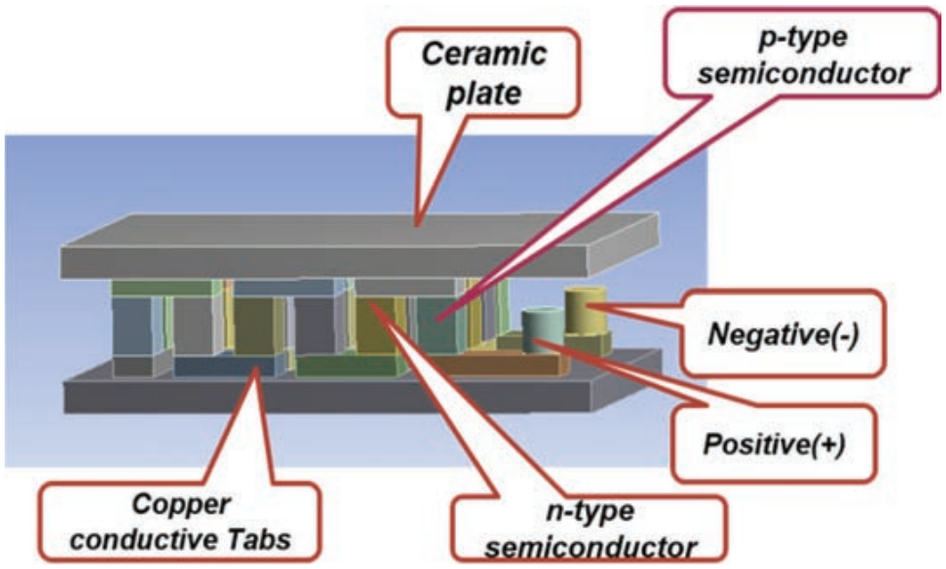

Figure 5. 3-D schematic of multielement TEG.

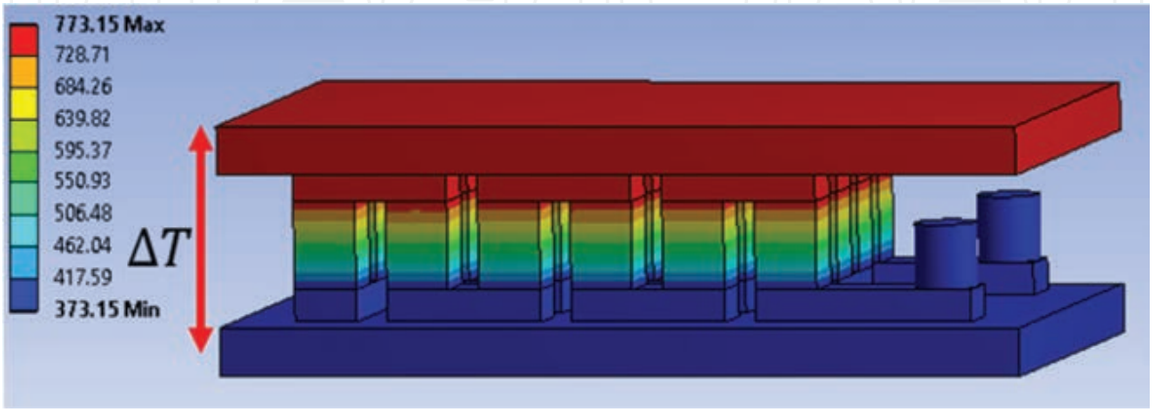

Figure 6. Temperature gradient within TEG.

After temperature gradient has been induced between hot and cold sides of TEG, voltage occurred on TEG-positive and -negative poles due to Seebeck effect, as depicted in **Figure 7**.

Voltage generated in TEG due to Seebeck effect induces the movement of charge carriers within p-and n-type semiconductor legs and, hence, electrical current in electrical circuit including load resistor R_L connected to TEG poles, current density formed, is displayed in **Figure 8**.

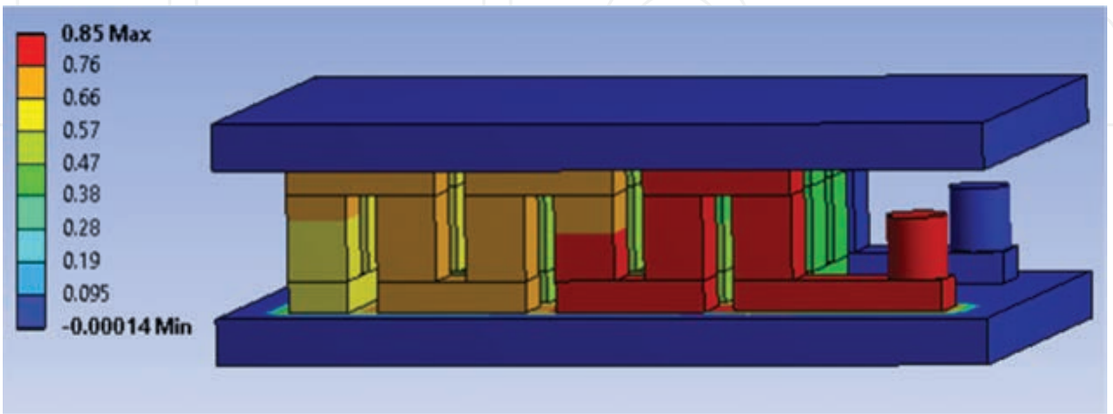

Figure 7. Voltage distribution within TEG.

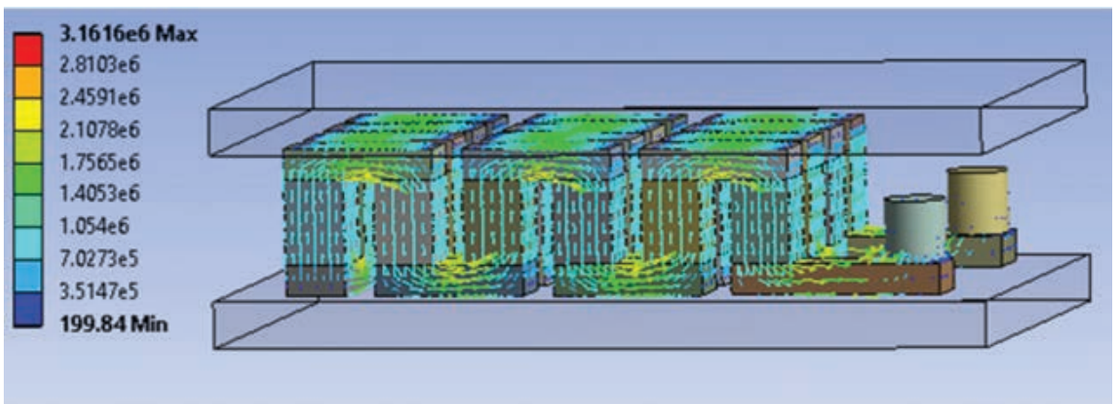

Figure 8. Current density within TEG.

3.2. 1-D representation of TEG

Establishing one-dimensional (1-D) representation of TEG is helpful in determining analytical expressions of heat absorbed and heat rejected, as the power output of TEG is defined as the difference between heat absorbed and heat rejected. **Figure 9** represents 1-D schematic of TEG with heat source and heat sink, respectively, applied on top and bottom sides of TEG.

T_H, Q_H, and K_H are, respectively, heat source temperature, heat supplied from heat source to TEG, and thermal conductance of hot side of TEG. T_L, Q_L, and K_L are, respectively, heat sink temperature, heat rejected from TEG to heat sink, and thermal conductance of TEG cold side. T_h and Q_h define the temperature of hot junction of thermocouples and heat flow through hot junctions of TEG. T_c and Q_c describe the temperature at cold junction of thermocouples and

http://dx.doi.org/10.5772/65741

heat flow through cold junctions of TEG. Assuming thermoelectric properties to be temperature independent, α, k, ρ can, respectively, be defined as constant Seebeck coefficient, constant thermal conductivity, and constant electrical resistivity.

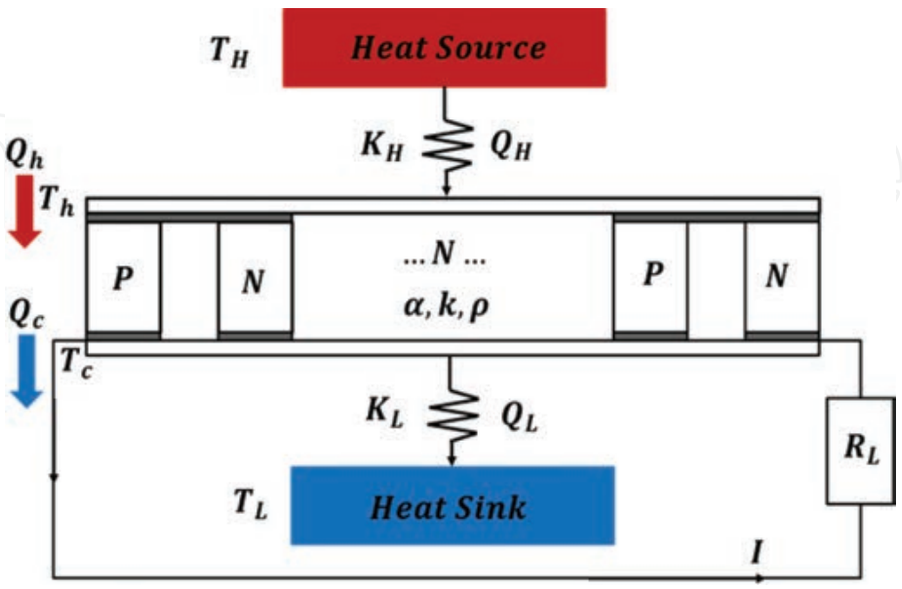

Figure 9. 1-D schematic of multielement TEG.

3.3. Electrical network resistance

Electrical resistance network of TEG is shown in **Figure 10**. P-type and n-type semiconductor legs are connected to each other electrically in series through copper-conductive tabs.

R_p and R_n are electrical resistance associated, respectively, with p- and n-type semiconductor legs. R_{cpeh}, R_{cpec}, and R_L are, respectively, electrical resistance of copper-conductive strips on the hot side, electrical resistance of copper-conductive strips on the cold side, and external load resistance.

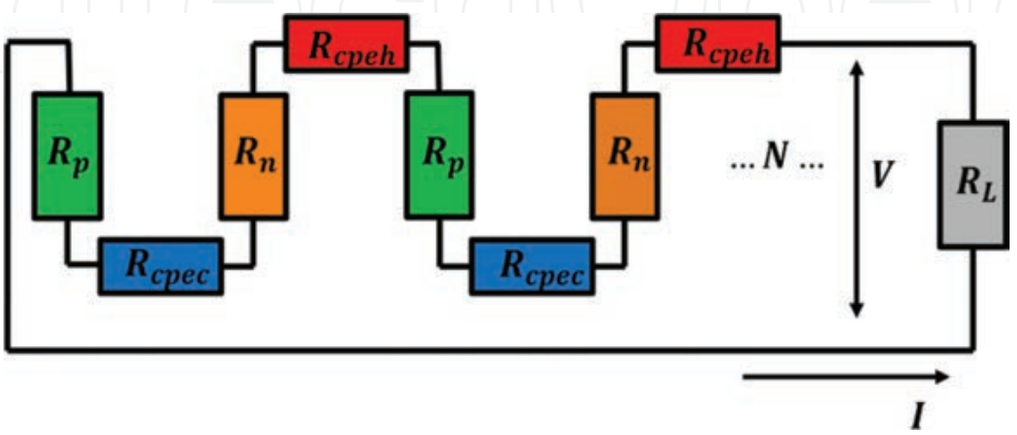

Figure 10. Electrical network resistance.

3.4. Thermal network resistance

Thermal resistance of TEG is shown in **Figure 11** and it assists in determining heat transfer rate through ceramic plates, copper strips, and p- and n-type semiconductor legs. The number of thermocouples is N.

T_{eceh}, T_{iceh}, and R_{ceh} are, respectively, external temperature of hot ceramic plate, internal temperature of hot ceramic plate, and thermal resistance associated with ceramic plate on the hot side. T_h, R_{cph}, and R_{teg} are, respectively, the temperature at the hot junction of p- and n-type semiconductor legs, thermal resistance of copper strip on the hot side, and thermal resistance of both p- and n-type semiconductor legs. T_c, R_{cpc}, and T_{icec}, are, respectively, the temperature at cold junction of p- and n-type semiconductor legs, thermal resistance of ceramic plate on the cold side, and internal temperature of cold ceramic plate. R_{cec} and T_{ecec} are, respectively, thermal resistance of cold ceramic plate and external temperature of cold ceramic plate.

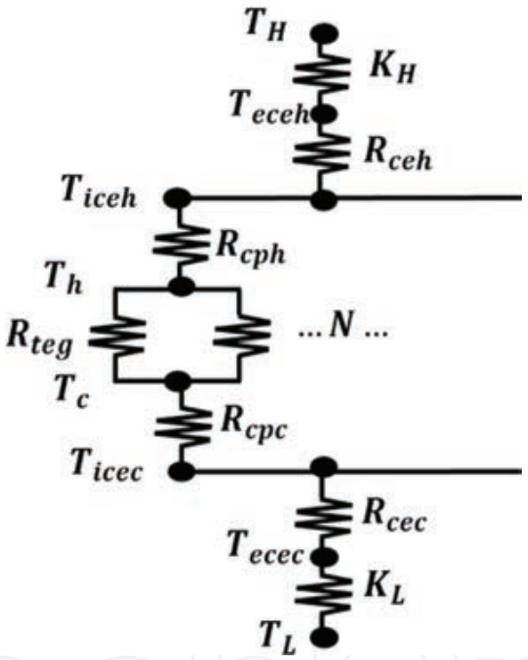

Figure 11. Thermal resistance network.

4. Theoretical model

4.1. Analysis of thermoelectric material properties and geometry of TEG

Thermoelectric materials of TEG legs, p- and n-type semiconductors, are characterized by parameter called the figure of merit Z, which measures the ability of thermoelectric materials to convert heat into electrical power. The figure of merit is expressed as follows:

$$Z = \frac{\alpha^2}{\rho k}, \tag{3}$$

http://dx.doi.org/10.5772/65741

where α, ρ, and k are, respectively, Seebeck coefficient, electrical resistivity, and thermal conductivity of thermoelectric materials. Great thermoelectric materials possess high Seebeck coefficient, low electrical resistivity, and low thermal conductivity [10].

In order to obtain maximum figure of merit, when designing TEG, the geometry of semiconductor legs and properties of thermoelectric materials need to satisfy the following equation [1, 11]:

$$\frac{A_p^2 L_n^2}{A_n^2 L_p^2} = \frac{k_n \rho_p}{k_p \rho_n}, \tag{4}$$

where A_p, A_n, L_p, L_n, k_p, k_n, ρ_p, and ρ_n are, respectively, the cross-sectional area, length, thermal conductivity, and electrical resistivity of p- and n-type semiconductor legs.

To reduce manufacturing costs, p- and n-type semiconductor legs are fabricated with the same geometry, that is, $A_p = A_n = A$, and $L_p = L_n = L$. Similarly, p- and n-type semiconductor legs are made of doped alloys to produce the same thermoelectric properties, that is, $\rho_p = \rho_n$, $k_p = k_n$, and $\alpha_p = -\alpha_n$ [12].

4.2. TEG performance analysis

In order to obtain expressions describing TEG performance, thermocouple built by legs of p- and n-type semiconductors is extracted from **Figure 9** and represented in **Figure 12**. **Figure 12** represents heat transfer within single thermocouple. The length and cross-sectional area of both p- and n-type semiconductor legs are equal and symbolize as L and A, respectively. The junction of thermocouple is fixed at thermal conducting and electrical-insulating ceramic plate.

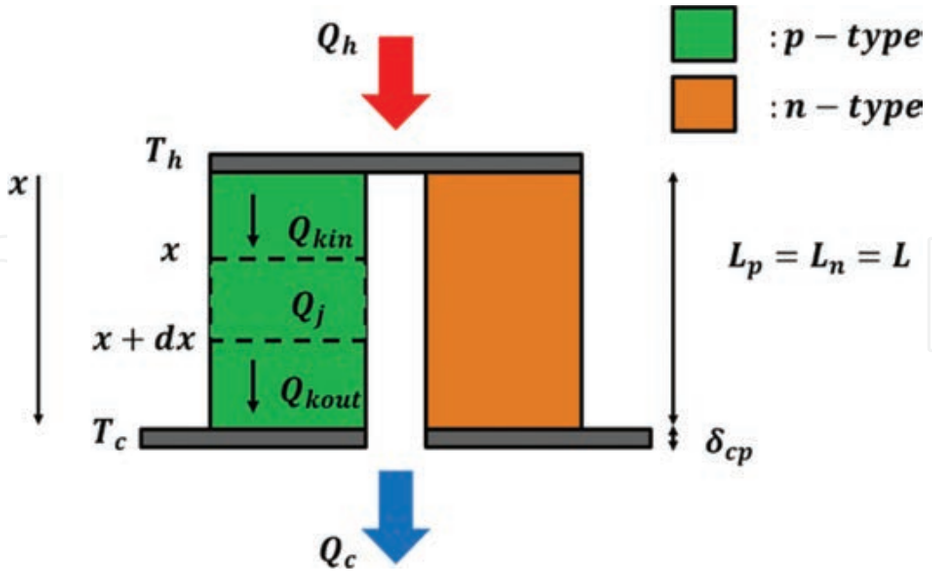

Figure 12. Heat transfer within TEG thermocouple.

Q_h, Q_c, Q_{kin}, Q_{kout}, Q_j, L_p, L_n, and δ_{cu} are, respectively, heat absorbed at hot junction, heat rejected at cold junction, Fourier heat conduction transferred inside of control volume, Fourier

heat conduction transferred out of control volume, Joule heating generated within control volume, the length of p- and n-type legs, and the thickness of copper electrical-conducting strips.

Employing the conservation of energy and assuming one-dimensional steady-state condition, the energy equation of differential control volume inside of p-type semiconductor leg can be expressed as follows:

$$Q_{\text{kin}} - Q_{\text{kout}} + Q_j = 0, \tag{5}$$

$$Q(x) - Q(x+dx) + Q_j = 0. \tag{6}$$

Using Taylor expansion:

$$Q(x) - \left(Q(x) + \frac{\partial Q(x)}{\partial x}dx\right) + \frac{I^2\rho_p}{A_p}dx = 0, \tag{7}$$

I represents electrical current induced within TEG device:

$$-\frac{\partial Q(x)}{\partial x}dx + \frac{I^2\rho_p}{A_p}dx = 0. \tag{8}$$

Fourier's law of conduction for one-dimensional heat conduction states:

$$Q(x) = -k_p A_p \frac{\partial T_p}{\partial x}. \tag{9}$$

Substituting Eq. (9) into Eq. (8):

$$-\frac{\partial}{\partial x}\left(-k_p A_p \frac{\partial T_p}{\partial x}\right)dx + \frac{I^2\rho_p}{A_p}dx = 0. \tag{10}$$

Provided that thermoelectric properties are temperature independent, k_p can be taken out of derivative and Eq. (10) can be expressed as follows:

$$k_p A_p \frac{d^2T_p}{dx^2}dx + \frac{I^2\rho_p}{A_p}dx = 0. \tag{11}$$

Integrating Eq. (11):

$$\int_0^x k_p A_p \frac{d^2T_p}{dx^2}dx + \int_0^x \frac{I^2\rho_p}{A_p}dx = 0, \tag{12}$$

$$k_p A_p \left(\frac{dT_p}{dx}|_x - \frac{dT_p}{dx}|_0\right) + \frac{I^2\rho_p}{A_p}x = 0, \tag{13}$$

$$x = 0 \rightarrow T_p(0) = T_h, \tag{14}$$

$$k_p A_p \frac{dT_p}{dx}\bigg|_0 = Q_p(0), \tag{15}$$

where $Q_p(0)$ is Fourier heat conduction transferred inside of top p-type leg:

http://dx.doi.org/10.5772/65741

$$\int_0^{L_p} k_p A_p \frac{dT_p}{dx} dx + \int_0^{L_p} \frac{I^2 \rho_p}{A_p} x dx = -\int_0^{L_p} Q_p(0) dx, \tag{16}$$

$$k_p A_p \left(T_p(L_p) - T_p(0) \right) + \frac{I^2 \rho_p}{A_p} \frac{{L_p}^2}{2} = -Q_p(0) L_p, \tag{17}$$

$$x = 0 \rightarrow T_p(0) = T_h, \tag{18}$$

$$x = L_p \rightarrow T_p(L_p) = T_c, \tag{19}$$

$$Q_p(0) = \frac{k_p A_p}{L_p} (T_h - T_c) - 0.5 \frac{I^2 \rho_p L_p}{A_p}. \tag{20}$$

Considering Peltier effect happening at the hot junction of p-type leg:

$$Q_{\text{ph}} = \alpha_p I T_h + \frac{k_p A_p}{L_p} (T_h - T_c) - 0.5 \frac{I^2 \rho_p L_p}{A_p}, \tag{21}$$

where Q_{ph} is the total heat absorbed at the hot junction of p-type leg.

Employing the same procedure with the same boundary conditions to derive heat flow through n-type leg leads to the expression of Q_{nh} as follows:

$$Q_{\text{nh}} = -\alpha_n I T_h + \frac{k_n A_n}{L_n} (T_h - T_c) - 0.5 \frac{I^2 \rho_n L_n}{A_n}, \tag{22}$$

where Q_{nh} is the total heat absorbed at the hot junction of n-type leg. The total heat absorbed at the hot junction of both p- and n-type semiconductor legs is, therefore:

$$Q_h = Q_{\text{ph}} + Q_{\text{nh}}, \tag{23}$$

$$Q_h = (\alpha_p - \alpha_n) I T_h + \left(\frac{k_p A_p}{L_p} + \frac{k_n A_n}{L_n} \right) (T_h - T_c) - 0.5 \left(\frac{\rho_p L_p}{A_p} + \frac{\rho_n L_n}{A_n} \right) I^2. \tag{24}$$

We use the same method to derive expression for heat rejected at the cold junction of p-type and n-type legs. Consequently, the following expression is obtained:

$$Q_c = (\alpha_p - \alpha_n) I T_c + \left(\frac{k_p A_p}{L_p} + \frac{k_n A_n}{L_n} \right) (T_h - T_c) + 0.5 \left(\frac{\rho_p L_p}{A_p} + \frac{\rho_n L_n}{A_n} \right) I^2. \tag{25}$$

4.3. TEG performance expressions

TEG is characterized by numerous performance expressions, including heat absorbed on the hot side, heat rejected on the cold side, power output, voltage induced, and current flowing in the electrical circuit with load resistor. Defining symbols below from Eqs. (24) and (25):

$$K = \frac{k_p A_p}{L_p} + \frac{k_n A_n}{L_n}, \tag{26}$$

$$r = \frac{\rho_p L_p}{A_p} + \frac{\rho_n L_n}{A_n}, \tag{27}$$

$$\alpha = \alpha_p - \alpha_n. \tag{28}$$

Expressions of heat flow through the hot and cold junctions for N semiconductor thermocouples can therefore be expressed as follows:

$$Q_h = N(\alpha I T_h - 0.5 r I^2 + K(T_h - T_c)), \tag{29}$$

$$Q_c = N(\alpha I T_c + 0.5 r I^2 + K(T_h - T_c)). \tag{30}$$

As stated previously, the power generated by TEG is defined as the difference between heat absorbed at the hot junction and heat rejected at the cold junction:

$$P = Q_h - Q_c = N(\alpha I(T_h - T_c) - r I^2). \tag{31}$$

Optimal current generated in TEG is obtained by first deriving Eq. (31) with respect to current as follows:

$$\frac{dP}{dI} = N(\alpha(T_h - T_c) - 2Ir). \tag{32}$$

Eq. (32) is equated to zero to determine the following expression of optimal current:

$$I_{\text{opt}} = \frac{\alpha(T_h - T_c)}{2r}. \tag{33}$$

Generally speaking, voltage, current, and output power induced in TEG consisting of set of thermocouples similar to the one represented in **Figure 9** are, respectively, defined as:

$$I = \frac{\alpha(T_h - T_c)}{r + R_L}, \tag{34}$$

$$P = I^2 R_L = \left(\frac{\alpha(T_h - T_c)}{r + R_L}\right)^2 R_L, \tag{35}$$

$$V = I R_L = \frac{\alpha(T_h - T_c)}{r + R_L} R_L, \tag{36}$$

where R_L, is the external resistance load. To get optimum electrical current induced, and output power generated in the electrical circuit with TEG consisting of set of thermocouples, external resistance needs to be equal to the total internal electrical resistance of p- and n-type semiconductor legs. The efficiency of TEG is given by:

http://dx.doi.org/10.5772/65741

$$\eta = \frac{P}{Q_h}. \tag{37}$$

In actual TEG, two thermoelectric materials are used, that is, p- and n-type semiconductors. The maximum efficiency provided by TEG is expressed as follows:

$$\eta_{\max} = \left(1 - \frac{T_h}{T_c}\right) \frac{\sqrt{1 + Z\overline{T}} - 1}{\sqrt{1 + Z\overline{T}} + \frac{T_h}{T_c}}, \tag{38}$$

where Z and $\overline{T}$ are, respectively, the figure of merit of p- and n-type semiconductors and averaged temperature between temperatures at the hot and cold sides.

4.4. Performance simulation example of a TEG

Numerical example is adopted in order to optimize and analyze effects of heat transfer governing equations on output power, efficiency, and induced voltage of TEG.

In numerical analysis, the following geometry is adopted (**Table 1**).

The following thermoelectric properties are adopted (**Table 2**).

Number of pairs (N)	Cross-sectional area (A)	Length (L)
10	$2.5 \times 2.5 \times 10^{-6}$ m^2	2×10^{-3} m

Table 1. Geometry of TEG.

α_p	α_n	$\rho_p = \rho_n$	$k_p = k_n$
$185 \times 10^{-6} V/K$	$-185 \times 10^{-6} V/K$	1.65×10^{-5}Ohm × m	$1.47 W/(mK)$

Table 2. Thermoelectric properties.

All obtained performance curves are computed at the hot-side temperature up to $T_h = 673$ K and the cold-side temperature of $T_c = 373$ K.

4.4.1. Power and efficiency as function of electrical current

By fixing the cold side at temperature $T_c = 373$ K and varying the hot-side temperature from 473 to 673 K with increment of 100 K, the power generated behaves as follow:

One can observe that the power as a function of current behaves as a parabola with optimum power value at specific current. **Figure 13** shows the existence of maximal current value, which corresponds to optimum power. Any current higher or lower than the maximum current value generates power output less than optimum power. Also, as temperature at the hot side increases, then power produced increases as well.

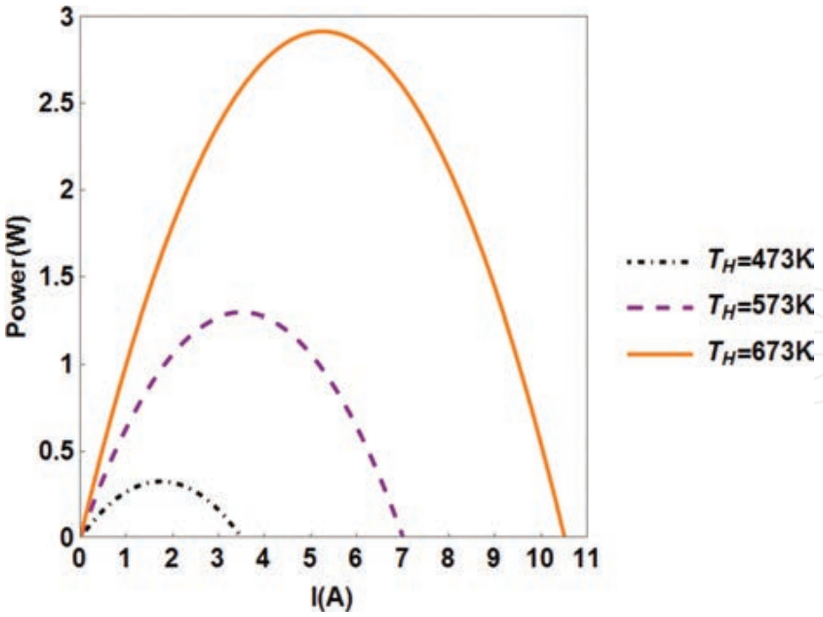

Figure 13. TEG output power as a function of electrical current.

Efficiency curves shown in **Figure 14** behave as parabola as well, with specific current value maximizing efficiency for each temperature difference. In real devices, TEGs are always operated at an optimal current. One thing to note is that the efficiency of TEG is still low compared to other energy-conversion techniques. A lot of effort has been made to enhance efficiency [13, 14]. Given that heat sources are plenty and free, TEGs could be promising solutions, when they are employed to harvest waste heat from industry activities and central-heating systems.

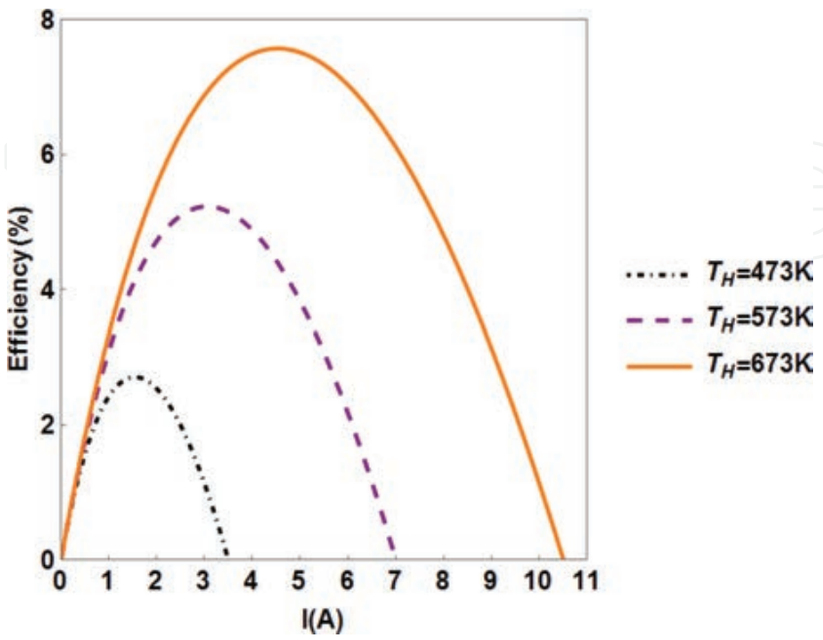

Figure 14. Efficiency as a function of current.

http://dx.doi.org/10.5772/65741

4.4.2. I-V dependences

Employing various temperature differences, while maintaining the cold-side temperature at 373 K, voltage induced as a function of current behaves as shown in **Figure 15**.

One can observe from **Figure 15** that voltage induced for each temperature difference is decreasing and the linear function of output electrical current. Slopes of I–V dependences are the same.

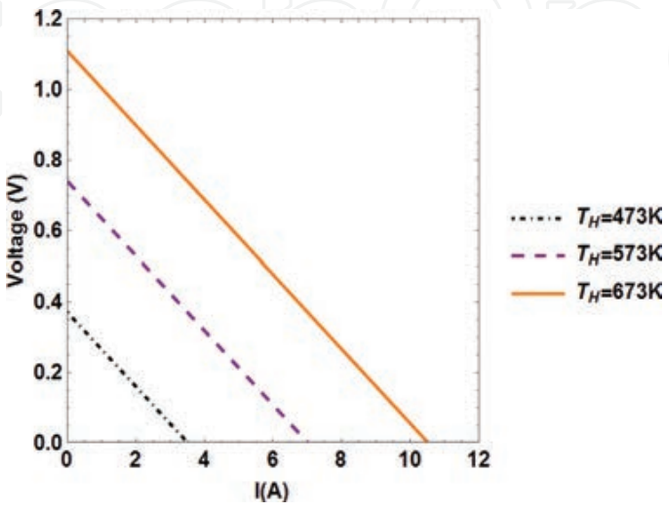

Figure 15. Voltage as a function of current (*I-V* dependences of TEG).

4.4.3. Power and efficiency as a function of hot-side temperature

While still maintaining the cold side at a temperature of 373 K and replacing current in output power equation (Eq. (31)) by optimal current expression (Eq. (33)), power expression becomes a function of temperature at the hot side, and **Figure 16** shows the behavior of output power as a function of the hot-side temperature.

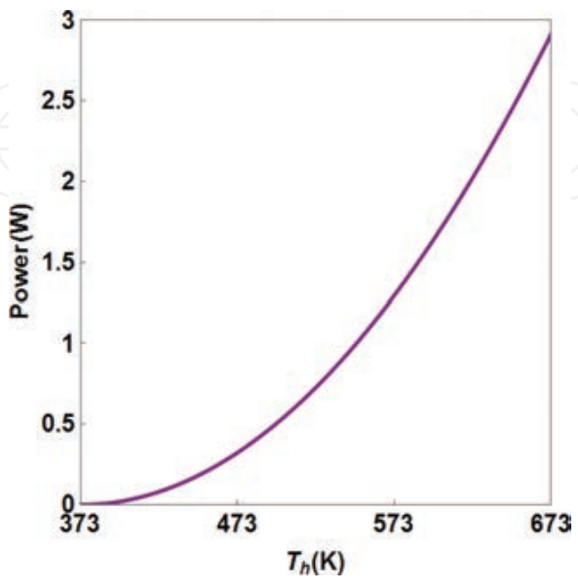

Figure 16. Power as a function of hot-side temperature.

Output power as a function of hot-side temperature behaves as nonlinear curve increasing as the hot-side temperature increases.

The efficiency of TEG as a function of hot-side temperature is shown in **Figure 17**.

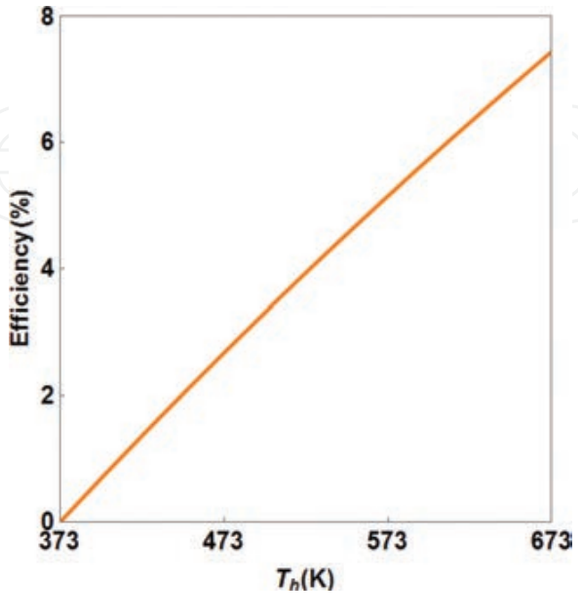

Figure 17. Efficiency of TEG as a function of hot-side temperature.

4.4.4. Power as a function of external load resistance

Figure 18 depicts variations of output power as a function of external load resistance. Eq. (35) is used to obtain dependences shown in **Figure 18**.

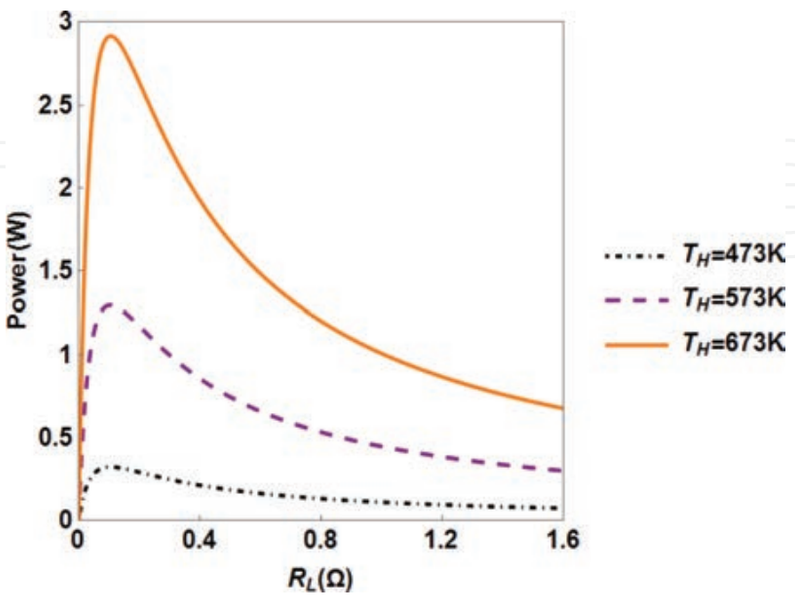

Figure 18. Output power as a function of external load resistance.

http://dx.doi.org/10.5772/65741

Optimal output power occurs when load resistance equates to internal electrical resistance of the total number of p- and n-type semiconductor legs.

4.4.5. Efficiency as a function of the figure of merit (ZT)

ZT value is modified figure of merit, where *T* represents averaged temperature between the hot-side and cold-side temperatures. For each temperature difference, efficiency increases as *ZT* value increases. Therefore, employing thermoelectric materials possessing high *ZT* values leads to great TEG efficiency (**Figure 19**).

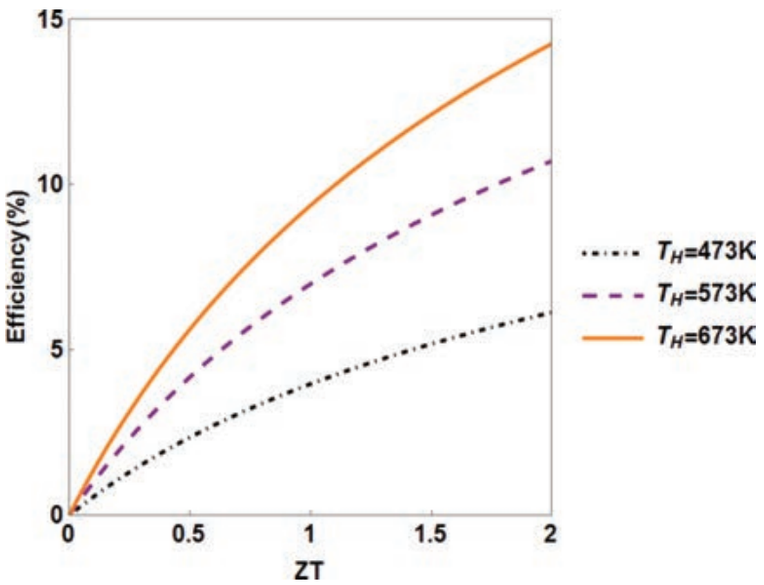

Figure 19. Efficiency as a function of *ZT* value.

5. Conclusion

In this chapter, the basics of thermoelectric generator devices are covered including phenomena that guide their operation. State-of-the-art modeling efforts are summarized. The presented modeling is crucial for comprehensive understanding of heat to electric energy conversion in TEGs. Simulation results are very useful in predicting the maximum ratings of TEGs during operation under different ambient conditions.

Acknowledgements

This work was funded by the startup fund from Virginia Polytechnic Institute and State University.

Author details

Eurydice Kanimba and Zhiting Tian*

*Address all correspondence to: zhiting@vt.edu

Virginia Polytechnic Institute and State University, USA

References

[1] Rowe DM. CRC handbook of thermoelectric, CRC press, Boca Raton, 1995.

[2] Rowe DM and Bhandari CM. Modern thermoelectrics, Prentice Hall, Upper Saddle River, 1983.

[3] Zevenhoven R and Beyene A. The relative contribution of waste heat from power plants to global warming. Energy, 2011. **36**(6): p. 3754–3762. DOI: 10.1016/j.energy.2010.10.010

[4] Moh'd AA-N, Tashtoush BM and Jaradat AA. Modeling and simulation of thermoelectric device working as a heat pump and an electric generator under Mediterranean climate. Energy, 2015. **90**: p. 1239–1250.

[5] Mamur H and Ahiska R. A review: Thermoelectric generators in renewable energy. International Journal of Renewable Energy Research (IJRER), 2014. **4**(1): p. 128–136.

[6] Ioffe A, Kaye J and Welsh JA. Direct conversion of heat to electricity. 1960: John Wiley and Sons, Inc.

[7] Sutton GW. Direct energy conversion, McGraw-Hill, New York, 1966.

[8] Decher R. Direct energy conversion: fundamentals of electric power production, Oxford University Press on Demand, Oxford, 1997.

[9] Riffat SB and Ma X. Thermoelectrics: A review of present and potential applications. Applied Thermal Engineering, 2003. **23**(8): p. 913–935. DOI: 10.1016/S1359-4311(03)00012-7

[10] Dziurdzia P. Modeling and simulation of thermoelectric energy harvesting processes, InTech Open Access Publisher, Croatia, 2011.

[11] Thomas JP, Qidwai MA and Kellogg JC. Energy scavenging for small-scale unmanned systems. Journal of Power Sources, 2006. **159**(2): p. 1494–1509. DOI: 10.1016/j.jpowsour.2005.12.084

[12] Meng F, Chen L, and Sun F. A numerical model and comparative investigation of a thermoelectric generator with multi-irreversibilities. Energy, 2011. **36**(5): p. 3513–3522. DOI: http://dx.doi.org/10.1016/j.energy.2011.03.057

[13] Ebling D, et al. Module geometry and contact resistance of thermoelectric generators analyzed by multiphysics simulation. Journal of Electronic Materials, 2010. **39**(9): p. 1376–1380. DOI: 10.1007/s11664-010-1331-0

[14] Priya S and Inman DJ. Energy harvesting technologies. Vol. 21, Springer, New York 2009.

IntechOpen

IntechOpen